Spinel ferrites of the quaternary system Cu-Ni-Fe-O: Synthesis and characterization

F. KENFACK, H. LANGBEIN*
Institute of Inorganic Chemistry, Dresden University of Technology, Dresden 01062, Germany

Published online: 21 April 2006

The decomposition of the freeze dried Cu(II)-Ni(II)-Fe(III) formate precursors at 1000°C in air yields complex oxides $Cu_xNi_{1-x}Fe_2O_{4\pm\delta}$ ($0 \leq x \leq 1$) with a cubic spinel structure. For $x < 0.7$, single phase spinels are formed at 1000°C. However, for $0.7 \leq x \leq 1$, Copper oxide (CuO) is identified as a second phase and the formation of a pure spinel phase requires an increase of the iron content in the mixture. For example, $Cu_{0.81}Ni_{0.1}Fe_{2.09}O_4$ is a single phase at 1000°C/air. Other single spinel phases $Cu_{0.5+y}Ni_{0.5-y-z}Fe_{2+z}O_{4\pm\delta}$, $0 \leq (y+z) \leq 0.5$, in the phase triangle $Cu_{0.5}Ni_{0.5}Fe_2O_4$–$CuFe_2O_4$–$Cu_{0.5}Fe_{2.5}O_4$ have been synthesized under special $p(O_2)$/T—synthesis conditions. The increase of the iron content requires an increase of the reaction temperature and/or a decrease of the $p(O_2)$ in the reaction gas stream. The oxygen exchange between $Cu_{0.9}Fe_{2.1}O_{4.02}$ and the reducing gaseous phases shows that the non stoichiometry δ of copper ferrite is only about ±0.03. Significant changes in the oxygen content lead to the separation in different phases. The electrical and magnetic properties of copper ferrite samples depend on their chemical composition and preparation conditions.

1. Introduction

The system Cu-Ni-Fe-O was first studied by Van Uitert [1]. One important finding of the author is that copper ferrite $CuFe_2O_4$ shows a tetragonal structure but with the addition of nickel, the tetragonality disappears and the copper-nickel ferrite samples exhibit a cubic structure. Since then, there has been remarkable other contributions such as Mössbauer studies [2, 3], cations distribution [4], electrical and magnetic properties [4, 5]. These previous works were based only on the spinel solid-solutions formed between $NiFe_2O_4$ and $CuFe_2O_4$. Moreover, the conventional ceramic method, requiring a working temperature above 1000°C, was commonly used. In the last decades, non-conventional soft chemistry routes such as the sol-gel method, the thermal decomposition of suitable complexes and coprecipitation method have been developed for the synthesis of ceramic materials. These methods are useful and attractive techniques because they allow the production of materials at a relatively low temperature [6].

Recently, reactive freeze-dried Cu–Fe formate precursors of appropriate compositions were used as starting powders for the synthesis of copper ferrites [7]. The thermal decomposition of these precursors ends already at about 400°C. Nevertheless, because of the intermediate reduction of Cu^{2+} to Cu by the carboxylate, a single phase copper ferrite can not be obtained. This leads to a phase separation and the full reaction to the complex oxide needs a temperature higher than 800°C. In order to bypass the reductive elimination of carboxylate ligands on the direct synthesis of a single spinel phase, mixtures of fine grained metals were used as starting materials [8]. The phase formation and the phase stability were investigated as a function of the temperature (800–1200°C) and the oxygen partial pressure (10^{-4}–1 bar). The authors found that for a given value of x, the synthesis of single phase spinel compounds $Cu_{1-x}Fe_{2+x}O_4$ ($0.1 \leq x \leq 0.5$) requires specific temperature—$p(O_2)$—conditions. Unlike the freeze dried Cu(II)–Fe(III) fomate, the thermal decomposition of the freeze dried Ni(II)–Fe(III) formate leads to the direct formation of nickel ferrite which becomes well crystalline around 800°C. On the other hand, the regeneration of $NiFe_2O_4$ from the taenite (γNi, Fe) phase is accomplished at 800°C [9]. This temperature is also 300°C below the temperature ($T \leq 1100$°C) employed when the mixtures NiO: α-Fe_2O_3 or Ni: 2Fe are the starting powders.

In what follows, we intend to use the freeze dried precursors Cu(II)–Ni(II)–Fe(III) formate as starting powders for the synthesis of different spinel solid-solutions.

*Author to whom all correspondence should be addressed.
0022-2461
DOI: 10.1007/s10853-006-6263-y

Furthermore, our attention is paid on the determination of the working conditions (T/p(O_2)) required for the synthesis and the stability of single spinel phases in the phase triangle $Cu_{0.5}Fe_2O_4$–$Cu_{0.5}Ni_{0.5}Fe_2O_4$–$CuFe_2O_4$. From the data existing in the literature, we establish for some examples the relation between the synthesis conditions and the physical properties of Cu–Ni ferrite materials.

2. Experimental

2.1. Synthesis

The formate precursors used for the preparation of Cu–Ni ferrites were obtained by the freeze drying method. The starting material, iron(II) formate, was prepared as described by Bonsdorf *et al.* [10]. The Ni(II) formate (0.19 M) and the Cu(II) formate (0.29 M) solutions were obtained by dissolving basic nickel carbonate and basic copper carbonate in appropriate amounts of formic acid, respectively. According to the desired composition of ferrite samples "$Cu_xNi_{1-x}Fe_2O_{4\pm\delta}$ $(0 < x < 1)$" and "$Cu_{0.5+y}Ni_{0.5-y-z}Fe_{2+z}O_{4\pm\delta(}$ $(0 \leq (y+z) \leq 0.5)$", adequate volumes of Cu(II) and Ni(II) formate solutions were mixed and the required amount of the solid Fe(II) formate was added. Upon stirring, Fe(II) formate was dissolved and Fe(II) was oxidized to Fe(III) with a twofold excess of H_2O_2. The resulting brown Cu(II)–Ni(II)–Fe(III) formate solutions were then frozen in liquid nitrogen and dried from -40° to 25°C in the vacuum chamber of a freeze drying apparatus (Alpha 2–4, Christ). After 72 h, the drying process was complete and loose, fine grained powders were obtained.

2.2. TG/DTA

The decomposition processes of the formate precursors were investigated by means of Netzsch Thermal Analyser STA 409 in air and in an argon 4.6 (AIR LIQUIDE, purity 99.996%) gas flow of 4.5 l/h. Because of the open gas outlet of the TG device, a slight air diffusion against the gas flow can not be excluded. The maximum p(O_2) in the environment of the sample carrier during the measurement in Ar atmosphere can be estimated as about 10^{-3} bar. This relatively low oxygen partial pressure allows the detection of primary gaseous and solid decomposition products and the slow oxidation of the primary solid products.

2.3. Phase analysis

The X-ray diffraction (XRD) measurements were performed at room temperature using a D5000 diffractometer (Siemens) with CuK_α radiation ($\lambda = 1.5406$ Å). The data were collected in the 2θ range of 10–80° with a step of 0.02° (the time was counted one second per step). For a quantitative analysis, the XRD data were collected in the 2θ range of 20–80° with a step of 0.01° (the time was counted 6 s per step). The phase identification was performed by comparing the measured diffraction pattern with those listed in the JCPDS database. The lattice parameters of compounds were estimated from the X-ray diffraction peak positions using the program WinXPOW [11].

2.4. Oxygen non-stoichiometry measurements

The initial oxygen stoichiometry of $Cu_{0.9}Fe_{2.1}O_{4\pm\delta}$, determined by the total reduction in H_2 atmosphere, was 4.02. That means the spinel must contain some cation vacancies. The amount of oxygen exchanged between $Cu_{0.9}Fe_{2.1}O_{4.02}$ and the gas flow at a given temperature/p(O_2) was determined using the solid-electrolyte technique employing a PC-controlled device OXYLYT (SensoTech Magdeburg, Germany) [12].

2.5. Electrical conductivity measurements

The electrical conductivity measurements of the samples were proceeded in air and in argon 4.6 atmosphere using a DC four-point method. The heating and the cooling processes were carried out between room temperature and 1223 K, with a rate of 5 K/min. At 1223 K, the equilibrium state values of the conductivity were achieved after 3–6 h. The knowledge of the exact geometry of the sample was necessary to calculate the conductivity from the resistance. From the recorded data, plots of the conductivity versus 1000/T were constructed.

2.6. Magnetic measurements

Weighed quantities (~25 mg) of oxide powders were introduced into a small cylindrical PVC-container (diameter: 4 mm; height: 4 mm). The measurements were carried out at 5 K and 300 K by using a vibrating sample magnetometer (Oxford Instruments) with nickel as a calibration substance.

3. Results and discussion

3.1. Characterization and thermal decomposition of freeze dried copper nickel iron formate precursors

Fig. 1 shows the XRD patterns of some freeze dried Cu(II)–Ni(II)–Fe(III) formate precursors. One notes that the amount of the crystalline component of the $Cu_xNi_{1-x}Fe_2$ formate in proportion to the amorphous phase becomes higher as the copper content "x" increases. In fact, when x is equal to 0.3, the precursor does not show any diffraction peak accounting for an amorphous state. For x equal to 0.5 and to 0.9, a small amount of the crystalline phase "$Cu(HCOO)_2$" is indexed beside the amorphous phase. The increase of the peaks intensity of the copper formate with the value of x is observed. It turns out that the segregation of some copper formate took place during the freeze drying process.

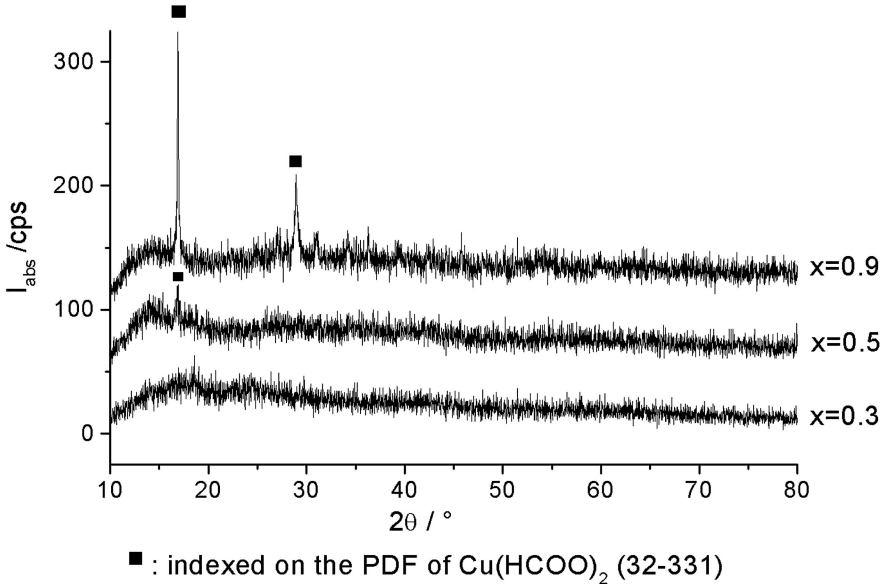

Figure 1 XRD patterns of freeze dried $Cu_xNi_{1-x}Fe_2$ formate precursors with $x = 0.3$, $x = 0.5$ and $x = 0.9$.

The thermal decomposition of the freeze dried Cu–Fe formate and Ni–Fe formate were investigated by thermal analysis and mass spectrometry methods [7, 9]. On the basis of the results of these previous studies, the thermal decomposition of the mixed Cu–Ni–Fe formates is evaluated. Fig. 2 shows the DTA- and TG-plots obtained in argon and air for the precursor $Cu_{0.5}Ni_{0.5}Fe_2$ formate, used as an example. These thermal analysis curves are compared with those of the freeze dried Ni(II)–Fe(III) formate and Cu(II)–Fe(III) formate [7, 9].

One notes that the TG profiles of the three precursors in argon atmosphere are rather similar. In a first step from room temperature up to about 180°C only water is released. Above 180°C the formate decomposition takes place. The decomposition of $Cu_{0.5}Ni_{0.5}Fe_2$ formate ends at 260°C whereas Cu(II)–Fe(III)- and Ni(II)–Fe(III) formate decompose completely at 290°C and 300°C, respectively. It turns out that the maximum mass loss of the mixed Cu(II)–Ni(II)–Fe(III) formate is reached at a temperature lower than that of the precursors Cu(II)–Fe(III)- and Ni(II)–Fe(III) formate. This means that during the thermal decomposition, an interaction takes place between the components and results in a lower decomposition temperature of the freeze-dried Cu(II)–Ni(II)–Fe(III) formate. As observed during the decomposition of *M*-formates and M-M′-formates (M, M′ = Cu, Ni, Fe) under argon atmosphere [7, 9], the main gaseous decomposition products identified using the mass spectroscopic analysis method are HCOOH and H_2CO (primary products), CO, CO_2 and H_2O (primary and secondary products) and H_2 (secondary product). The simultaneous release of HCOOH and CO_2 enhances the reductive decomposition of M-formate. The decomposition of the complex Cu–Ni–Fe formates is a superimposition of processes already described in [7, 9] for the single and binary formates. The small gain of mass above 280°C after decomposition in argon atmosphere allows the conclusion that lower oxidation states of the metals are formed during the primary process of decomposition. The 3% gain of mass correlates with the reception of about one oxygen per formula unit ("$Cu_{0.5}Ni_{0.5}Fe_2O_3 \rightarrow Cu_{0.5}Ni_{0.5}Fe_2O_4$"). The $p(O_2)$ of about 10^{-3} bar in the gas flow is sufficient for the end of this process within the measuring time. In air atmosphere (Fig. 2, curves d), the altogether exothermic consecutive processes of primary products result in a fast formation of CO_2 and H_2O and solid oxides which contain only Cu(II), Ni(II) and Fe(III). This process is already finished at 230°C. The 2% difference in the mass loss in Ar and air is caused by the different content of water in both measured samples (in dependence on the atmospheric humidity the water content of the samples can be somewhat different).

3.2. Phase formation

During the thermal treatment of the freeze dried precursor $Cu_{0.5}Ni_{0.5}Fe_2$ formate, the individual decomposition of Cu(II) formate results in the intermediate formation of copper metal (Fig. 3). As already observed during the synthesis of copper ferrite from the formate precursors [7], this should prevent the direct formation of a single spinel phase at a low temperature. On the other hand, no traces of nickel are detected on the XRD pattern obtained up to 260°C (Fig. 3). Two reasons may be responsible: the decomposition of nickel(II) formate and iron(III) formate take place simultaneously and inhibits the formation of nickel metal or the nickel metal is present but in an amorphous state [9]. Neither the first nor the second reason can be excluded. Perhaps, the less crystalline spinel formed already at 250°C is a nickel containing magnetite, $Ni_xFe_{(3-x)}O_4$.

The freeze dried precursors $Cu_xNi_{1-x}Fe_2$ formate with $x = 0.3$, 0.5, 0.6, 0.7 and 0.9 were decomposed in air

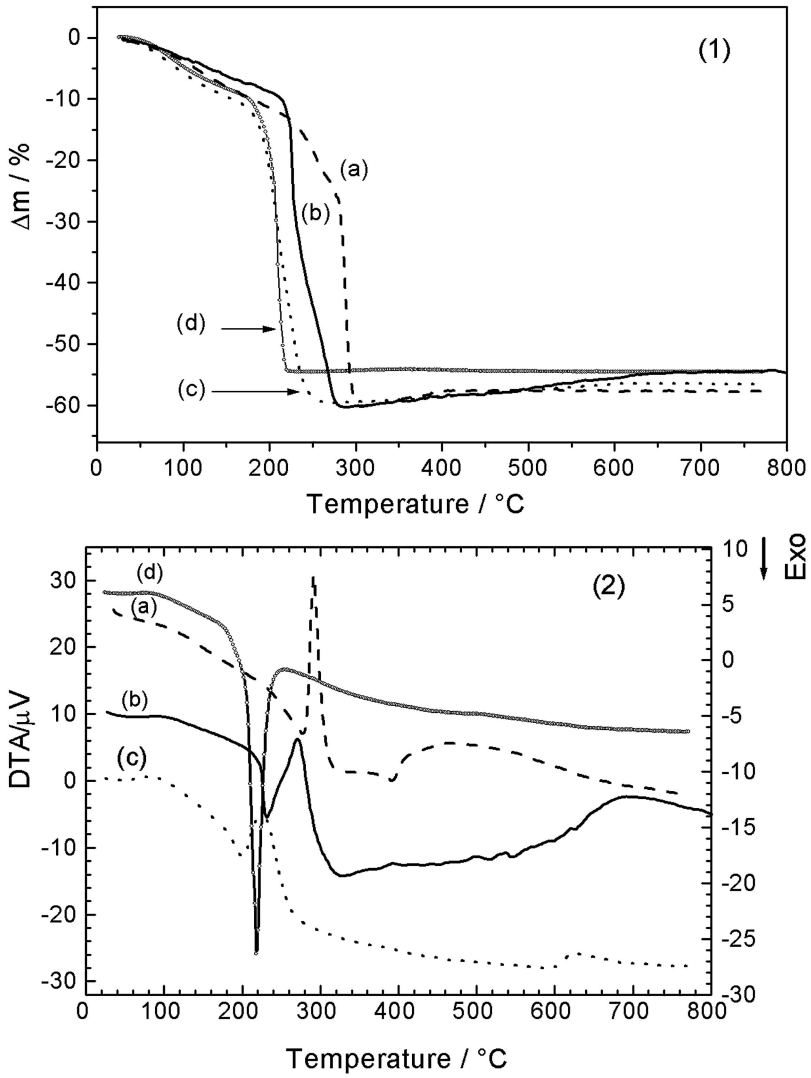

Figure 2 (1) TG- and (2) DTA-plots of freeze dried formate precursors: (a) $NiFe_2$ formate, (b) $CuFe_2$ formate and (c) $Cu_{0.5}Ni_{0.5}Fe_2$ formate, atm.: Ar, heating rate: 5 K/min; (d) $Cu_{0.5}Ni_{0.5}Fe_2$ formate, atm.: air, heating rate: 5 K/min.

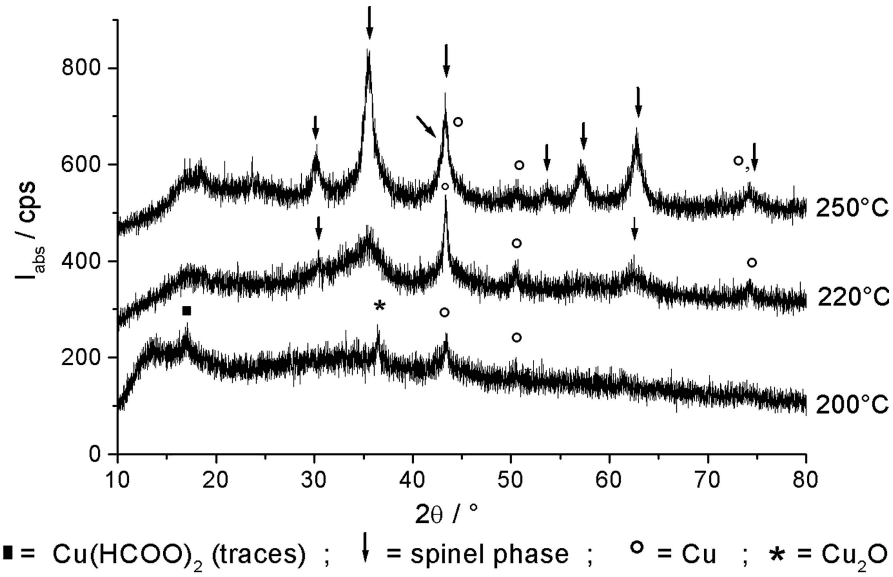

Figure 3 XRD patterns of the decomposition products of the freeze dried $Cu_{0.5}Ni_{0.5}Fe_2$ formate quenched after annealing up to 200°C, 220°C and 250°C, atm.: Ar; heating rate: 5 K/min.

at 400°C for three hours. To avoid an overheating of samples, because of the exothermic oxidation processes (see 3.1), the heating rate up to 400°C was 5 K/min and the decomposition was proceeded in thin layers on stainless steel plates. After this decomposition, the samples were pressed in pellets before being heated at different temperatures for 24 h. To maintain a single-phase spinel after synthesis at 1000°C, it was necessary to quench the material (by removing the sample from the furnace and cooling down to room temperature inside a desiccator). Fig. 4

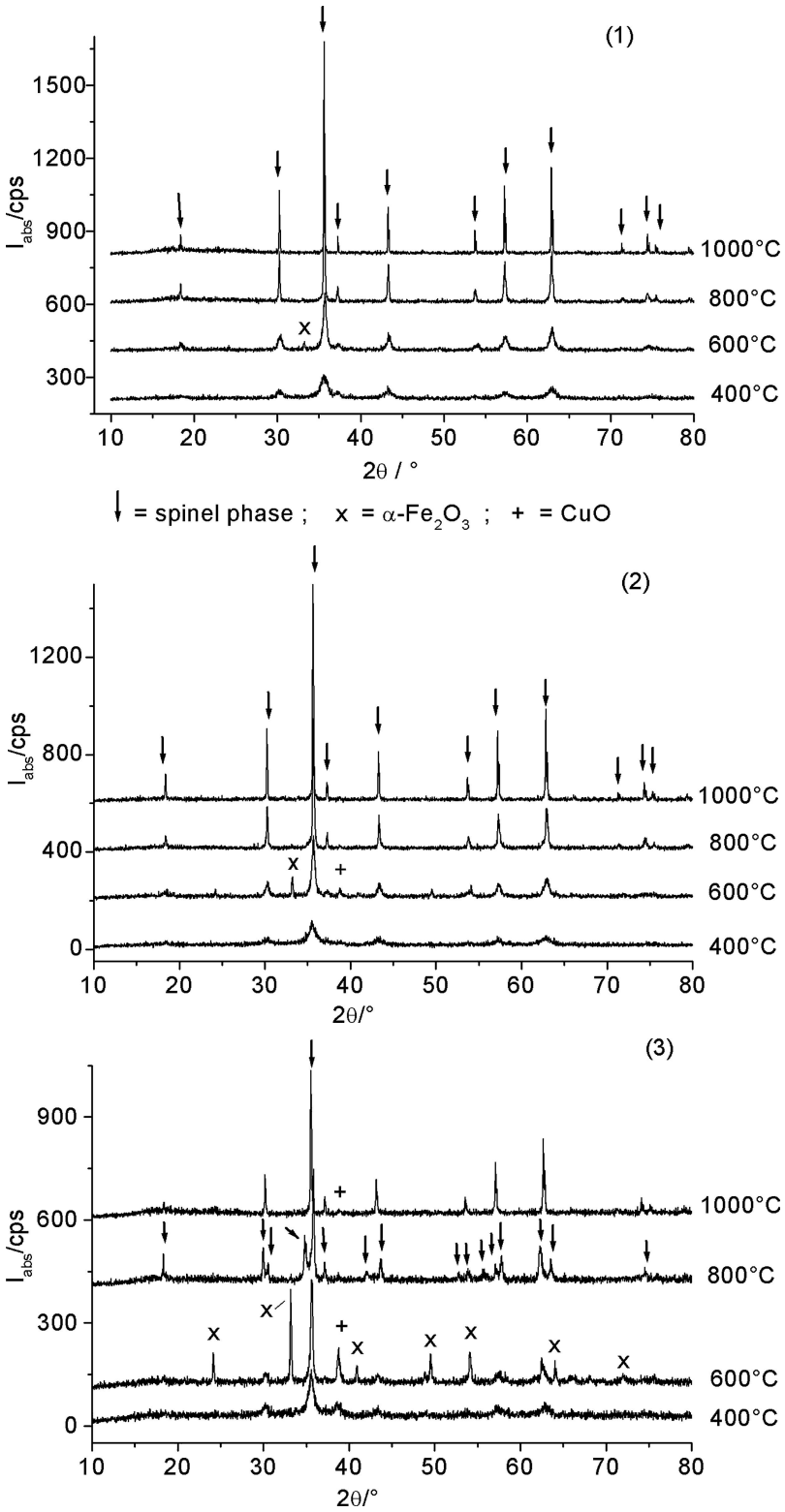

Figure 4 XRD patterns of the decomposition products of $Cu_xNi_{1-x}Fe_2$ formate annealed at 400°C and heated at different temperatures. (1) $x = 0.3$, (2) $x = 0.5$, (3) $x = 0.9$; atm.: air.

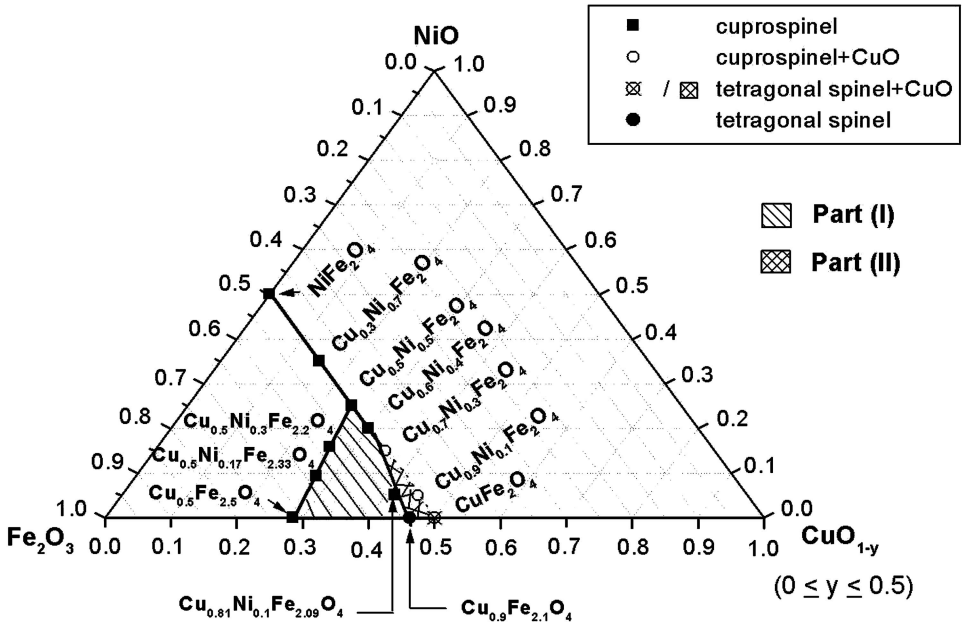

Figure 5 Formation of ferrites in the Cu–Ni–Fe–O system.

illustrates the XRD patterns of the samples with $x = 0.3$, 0.5 and 0.9.

After decomposition at 400°C the products contain a partially crystalline spinel phase. The compositions with $x = 0.3$ and $x = 0.5$ are single spinel phases. For other compositions, a very small amount of copper oxide (CuO) is identified. Upon heating up to 600°C, the crystallization of the spinel phase is enhanced. For the sample with $x = 0.3$, a small amount of α-Fe_2O_3 is formed whereas for other compositions both CuO and α-Fe_2O_3 are identified as second phases. It is important to mention that the presence of nickel oxide is not very well identified because the most intense peaks of NiO are covered by those of the spinel phase. Upon heating at 800°C, the amount of the spinel phase increases due to the reaction occurring between the single oxides (CuO/NiO and α-Fe_2O_3). For $x = 0.3$, 0.5, 0.6 and 0.7, the XRD patterns match with that of $NiFe_2O_4$ (cubic phase) whereas reflections arising due to the tetragonal $CuFe_2O_4$ are identified on the pattern of the sample with $x = 0.9$. After synthesis at 1000°C/air, the compositions with $x < 0.7$ are single spinel phases. For the compositions with $x \geq 0.7$, a very small amount of copper oxide (CuO) is identified. The separation of small amounts of CuO in air atmosphere at 1000°C is caused by the formation of a Cu(I) containing iron rich spinel. That means, the formation of a pure spinel phase should require an increase of the iron content in the mixture. Such behaviour is already known for spinel compounds $Cu_{1-x}Fe_{2+x}O_4$ [8]. It was found that single phase spinels with $x = 0.1$ and 0.2 can be synthesized at 1000°C in air. The synthesis of single phase spinels with $x > 0.2$ requires an increase of the synthesis temperature and/or a decrease of the oxygen partial pressure. Similar synthesis conditions should be expected for spinel compounds in the phase triangle $Cu_{0.5}Ni_{0.5}Fe_2O_4$–$CuFe_2O_4$ –$Cu_{0.5}Fe_{2.5}O_4$ ($Cu_{0.5+y}Ni_{0.5-y-z}Fe_{2+z}O_{4\pm\delta}$) (Fig. 5). To probe this assumption and to compare it with synthesis conditions found in [8], some mixed copper nickel ferrites were synthesized from freeze-dried Cu(II)–Ni(II)–Fe(III) formate precursors. The spinel phases $Cu_{1-x}Fe_{2+x}O_4$ (x = 0.1, 0.2, 0.33, 0.4 and 0.5) were prepared by solid state reactions using metallic precursors as described elsewhere [8]. Table I shows the synthesis conditions enabling the formation of the pure spinel phases and the lattice parameters of investigated compositions. It can be seen that the required synthesis temperature is ≥1000°C. At this temperature the advantage of the reactive carboxylate precursor is lost and a comparison between samples prepared from different precursors should be allowed.

After the decomposition of the appropriate freeze dried Cu(II)–Ni(II)–Fe(III) formate precursor at 400°C (3 h) followed by the annealing at 1000°C (24 h) in air, a pure spinel phase is obtained for the composition $Cu_{0.81}Ni_{0.1}Fe_{2.09}O_4$. For the solid solutions existing between the compositions $Cu_{0.5}Fe_{2.5}O_4$ and $Cu_{0.5}Ni_{0.5}Fe_2O_4$, the synthesis conditions enabling the formation of the pure spinel phases are similar to the conditions established in [8] for the preparation of iron-rich copper ferrites with the same iron content. This is shown in Table I for $Cu_{0.5}Ni_{0.3}Fe_{2.2}O_4$ and $Cu_{0.5}Ni_{0.17}Fe_{2.33}O_4$. The higher Cu(I)/Cu(II)—ratio in the appropriate Cu–Ni–Fe-spinels requires a somewhat higher synthesis temperature at the same $p(O_2)$. It is also shown in Table I that the nickel substitution leads to a slight decrease of the lattice parameter "a" of the ferrite sample.

Concerning the temperature-$p(O_2)$ conditions required for the synthesis of iron-rich copper nickel ferrites, the phase triangle $Cu_{0.5}Ni_{0.5}Fe_2O_4$–$CuFe_2O_4$ –$Cu_{0.5}Fe_{2.5}O_4$ can be subdivided in two main parts (Fig. 5). For compositions close to the section

TABLE I Synthesis conditions and characterization of complex oxides $Cu_{0.5+y}Ni_{0.5-y-z}Fe_{2+z}O_4$

Metal ion ratio (M:Fe with M = Ni, Cu)	Sample	Synt. temp (°C), atm	Phases composition	a (pm)
0.91:2.09	$Cu_{0.81}Ni_{0.1}Fe_{2.09}O_4$	1000, air	cSp	838.4
0.9:2.1	$Cu_{0.9}Fe_{2.1}O_4$	1000, air	tSp	584.7 (c = 858.9)
0.8:2.2	$Cu_{0.5}Ni_{0.3}Fe_{2.2}O_4$	1000, air	cSp + α-Fe_2O_3	–
		1100, air	cSp	836.3
		1100, argon 4.6 + 1% O_2	cSp	838.3
	$Cu_{0.8}Fe_{2.2}O_4$	1000, air	cSp	839.5
		1000, argon 4.6 + 1% O_2	cSp	840.0
0.67:2.33	$Cu_{0.5}Ni_{0.17}Fe_{2.33}O_4$	1000, air	cSp + α-Fe_2O_3	–
		1100, argon 4.6 + 1% O_2	cSp	839.3
	$Cu_{0.67}Fe_{2.33}O_4$	1000, air	cSp + α-Fe_2O_3	–
		1100, argon 4.6 + 1% O_2	cSp	840.2
0.5:2.5	$Cu_{0.5}Fe_{2.5}O_4$	1110, argon 4.6	cSp	841.1

(Synt. Temp (°C), atm = synthesis temperature, synthesis atmosphere; cSp = cupro-/cubic spinel; *t*Sp = tetragonal spinel)

$Cu_{0.6}Ni_{0.4}Fe_2O_4$–$Cu_{0.9}Fe_{2.1}O_4$ single phase spinels can be synthesized at 1000°C in air atmosphere; for compositions of part (I), the increase of the iron content requires an increase of the reaction temperature and/or a decrease of the $p(O_2)$ in the reaction gas stream; (b) in the second and small part (II), the partial reduction of Cu^{2+} to Cu^+ occurring above 800°C in air has an influence on the formation of a pure spinel phase. Consequently, copper oxide (CuO) appears as second phase. The synthesis of single phase spinels should require a low synthesis temperature and a high $p(O_2)$. Starting from a reactive carboxylate precursor, 70 h of heating at 800°C in the presence of pure oxygen is required for the synthesis of a pure copper ferrite phase "$CuFe_2O_4$". The same synthesis conditions should be applied for the preparation of other compounds appearing in the triangle (II).

3.3. Characterization

3.3.1. Iron rich copper ferrites "$Cu_{1-x}Fe_{2+x}O_4$" with x = 0.1, 0.2, 0.33, 0.4 and 0.5

Thermal stability. The composition of a non-stoichiometric spinel phase can be denoted as $AB_2O_{4\pm\delta}$. In the case of large changes in the oxygen content (δ), the spinel can form few distinctive different phases. This indicates that the study of the interaction of ferrites with the gas phase is crucial for the understanding of their properties.

In our previous work [8] on the influence of the temperature and the oxygen partial pressure on the phase formation in the system Cu–Fe–O, the synthesis and the thermal stability of copper ferrite samples "$Cu_{1-x}Fe_{2+x}O_4$ (x = 0.1, 0.2, 0.33, 0.4 and 0.5)" were performed at different temperatures (800–1200°C) and oxygen partial pressures ranging from 1.013×10^2 to 0.21×10^5 Pa. In the present study, the main objective is to establish the consequences resulting from the oxygen exchange between copper ferrite and the gaseous phase at different temperatures. For these experiments, the starting material used is a single tetragonal spinel phase "$Cu_{0.9}Fe_{2.1}O_{4.02}$" prepared in air at 1000°C (24 h) and cooled down to room temperature inside a desiccator (see Table I, [8]). The oxygen release of the oxide was measured on powders (50–100 mg) placed in a quartz container within the furnace of the solid electrolyte employing a PC-controlled device OXYLYT. From the recorded data, the variation of the oxygen stoichiometry as function of lg $p(O_2)$ at different temperatures is deduced (Fig. 6).

Under a given $p(O_2)$ of investigation, the sample $Cu_{0.9}Fe_{2.1}O_{4.02}$ is characterized by a drastic decrease of the oxygen content with the increase of the temperature. From the analysis of the XRD patterns of products obtained at the end of each measurement, the observed behaviors are due to the decomposition of the spinel phase. At 800°C, the reduction of Cu^{2+} to Cu^+ enhances the formation of cuprous ferrite (cubic spinel phase $Cu_{0.9-y}Fe_{2.1+y}O_{4.02-z}$) and delafossite, $CuFeO_2$. As the temperature increases, the reduction process becomes more important. Consequently, at 900°C the total dissociation of the cubic phase takes place and leads to the formation of delafossite and hematite (reaction 1).

$$Cu_{0.9}Fe_{2.1}O_{4.02} \xrightarrow{900^\circ C} 0.9CuFeO_2 + 0.6Fe_2O_3 + 0.21O_2 \quad (1)$$

Above 900°C, the reduction of α-Fe_2O_3 into Fe_3O_4 begins. The delafossite phase becomes unstable and its partial decomposition leads to the formation of Cu_2O which reacts progressively with Fe_3O_4. From this last process, a copper poor spinel phase is formed. It turns out that during the thermal treatment at a oxygen partial pressure lower than the coexistence pressure of the appropriate copper ferrite significant changes in the oxygen content lead to the separation in different phases.

Physical properties. From the results obtained above and according to [8], a modification of the conditions required for the synthesis of copper ferrite samples "$Cu_{1-x}Fe_{2+x}O_{4\pm\delta}(0 \le x \le 0.5)$" leads to a change of the oxygen stoichiometry and possibly, of the separation in different phases. These changes should also affect the nature of charge carrier and their concentration. For

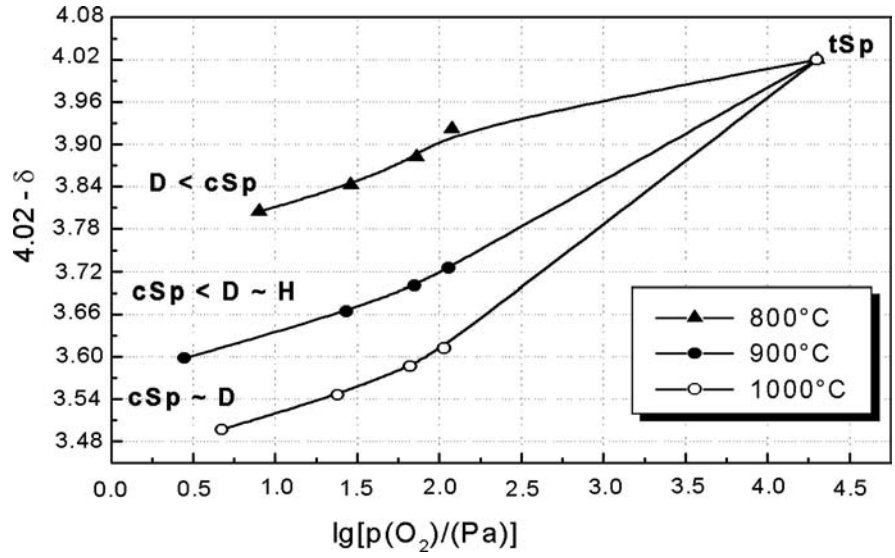

Figure 6 Total oxygen content in "$Cu_{0.9}Fe_{2.1}O_{4.02-\delta}$" as a function of $p(O_2)$ and T. (H = hematite, D = delafossite, cSp = cubic spinel, tSp = tetragonal spinel).

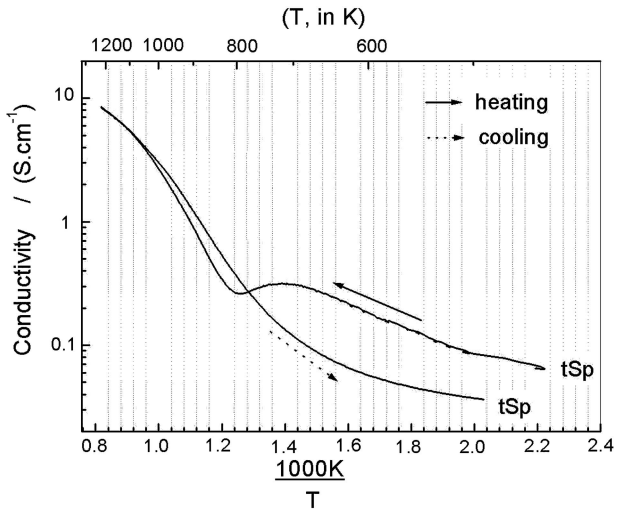

Figure 7 lg (σ) versus (1000/T) of the sample $Cu_{0.9}Fe_{2.1}O_{4.02}$. Heating and cooling rates: 5 K/min; atm.: air.

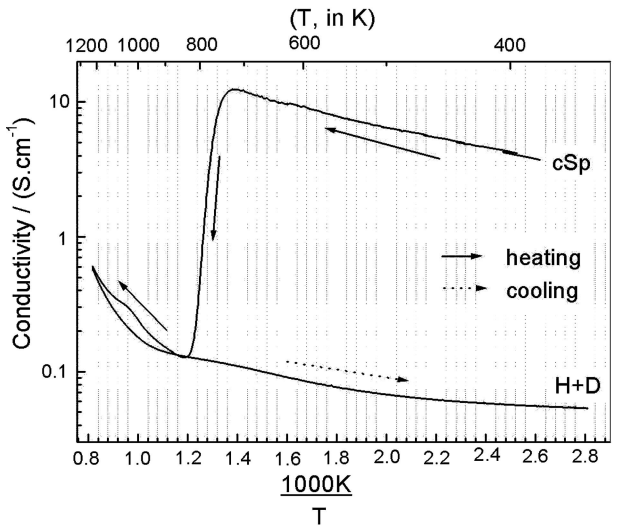

Figure 8 lg (σ) versus (1000/T) of the samples $Cu_{0.5}Fe_{2.5}O_{4\pm\delta}$. Heating and cooling rates: 5 K/min; atm.: Ar 4.6.

copper containing spinel ferrites, *n*- or *p*-conductivity is found in dependence on the synthesis conditions and the composition [13–15]. In order to eradicate the influence of the working atmosphere beside that of the temperature, the electrical conductivity of the selected samples $Cu_{0.9}Fe_{2.1}O_{4.02}$ and $Cu_{0.5}Fe_{2.5}O_{4\pm\delta}$ was measured preferentially under surrounding atmospheres identical to those used for their synthesis (i.e air and argon 4.6 gas flow, respectively). In Figs 7 and 8, heating and cooling plots of lg (σ) versus (1000/T) are displayed.

For both samples, the change in the conductivity with the temperature is not reversible. The conductivity of $Cu_{0.9}Fe_{2.1}O_{4.02}$ increases gradually with the temperature up to 733 K where a local broad maximum is observed (Fig. 7). Because heating and cooling curves are not identical, the observed anomaly is likely to be attributed to the thermal history of the sample rather than the change of the magnetic ordering in the ferrite lattice, as mentioned for $CuFe_2O_4$ [16, 17]. After synthesis at 1000°C, an equilibrium should exist between the copper ferrite and the surrounding air atmosphere. During the cooling process, a cubic to tetragonal transition takes place and the substance absorbs some oxygen. This results in the oxidation of some Cu^{1+} to Cu^{2+} and in the formation of a spinel with cation vacancies. Because of the fast cooling process, the oxygen stoichiometry of $Cu_{0.9}Fe_{2.1}O_{4.02}$ corresponds to a higher temperature equilibrium state. Due to this fact, some further oxidation of Cu^{1+} sets in between 700 and 800 K during the slow heating process and (in spite of the increase of the charge carrier mobility) the conductivity decreases because of the decreasing charge carrier concentration. Above 800 K, an equilibrium should be

reached and the further temperature dependence of the conductivity is the result of a superimposition of the actually increasing charge carrier concentration (formation of Cu^{1+} by oxygen delivery) and the increase of the charge carrier mobility. This point of view is confirmed by the non linear variation of the conductivity (σ) with the reciprocal temperature during the cooling process. Because of the slow cooling process (5 K/min), the room temperature conductivity now corresponds to a lower temperature equilibrium state in comparison with the quenched sample. The discussion of the anomalous conductivity behaviour corresponds with a *n*-type conductivity of the sample. Deeper informations would require isostoichiometric measurements [18].

For the composition $Cu_{0.5}Fe_{2.5}O_{4\pm\delta}$, the "high" conductivity value of ~12.5 S cm^{-1} registered at 720 K falls suddenly to 0.13 S cm^{-1} at 843 K (Fig. 8). On the XRD pattern of the slowly cooled pellet, the identified phases are delafossite ($CuFeO_2$) and hematite (α-Fe_2O_3). This result confirms once more the low stability of copper ferrites. Additional investigations performed on the samples with the composition $Cu_{0.67}Fe_{2.33}O_{4\pm\delta}$ and $Cu_{0.6}Fe_{2.4}O_{4\pm\delta}$ lead to the same conclusion.

For further considerations, the magnetic properties of copper ferrite samples "$Cu_{1-x}Fe_{2+x}O_4$ with $x = 0.1$, 0.2, 0.33, 0.4 and 0.5", which depend on the composition but also on the thermal history of the material, were determined. From the data presented in the Table II, it follows that at 5 K, the value of σ_S increases with the iron content x. Furthermore, the lattice parameter "a" also increases with x (Table II). For a fixed metal ion ratio, the lattice parameter "a" of the single spinel phase synthesized at a given temperature increases when the oxygen partial pressure during the synthesis decreases (case of the sample $Cu_{0.8}Fe_{2.2}O_4$, Table I). This is understandable because some Cu^{2+} with the smaller ionic radius is being replaced by Cu^{+} with a larger radius.

According to a number of investigators, it has been established that Cu^{+} ions have a strong preference for tetrahedral sites. On the other hand, the outer electron-shell of Cu^{+} is saturated, thereby leading to the magnetic moment of zero. From these two main remarks, the increase of the Cu^{+} ions content in the ferrite compound should enable the decrease of the magnetic moment of ions in the tetrahedral sites. It turns out that at 5 K, the increase of σ_S with the increase of x is mainly a consequence of the increase of iron ions content in the octahedral sites. The n_B-values given in Table II are somewhat lower than the values calculated using the formula $n_B = gS$ (with $g = 2$ and S is the spin state) for samples with Cu^{1+} and Cu^{2+} only on tetrahedral and octahedral sites, respectively. Already some other distribution caused by thermal site change processes or by oxidation during the cooling process could explain the small deviations. Because of the large importance of these both processes, a large influence of the synthesis conditions on the magnetic properties must be expected. It is already known for a long time that the saturation magnetization σ_S of "$CuFe_2O_4$" is greater after quenching than after slow cooling. This effect is mostly discussed in terms of different inversion degrees because of the relatively low activation energy of site exchange processes of Cu^{2+}-ions [4, 19]. Using the simple formula given above we can calculate $n_B = 1$ for a stoichiometric copper ferrite of the composition $[Fe^{3+}]_A[Cu^{2+}Fe^{3+}]_BO_4$. A decrease of the inversion degree would result in an increase of σ_S and n_B. According to our results given in [8] and above, different σ_S-values could be caused mainly by increasing stoichiometry deviations with the increase of synthesis temperature and/or cooling rate. The highest Cu: Fe ratio of a single phase spinel synthesized by us at $\theta \geq 1000$°C in air is 0.9:2.1. For the composition $[Cu^{1+}_{0.1}Fe^{3+}_{0.9}][Cu^{2+}_{0.8}Fe^{3+}_{1.2}]O_4$ $n_B = 2.3$ can be calculated. After the fast cooling process in air a composition "$Cu_{0.9}Fe_{2.1}O_{4.02}$" results. For a cation distribution $[Cu^{1+}_{0.06}Cu^{2+}_{0.04}Fe^{3+}_{0.9}][Cu^{2+}_{0.8}Fe^{3+}_{1.2}]O_{4.02}$ a little changed n_B—value of 2.26 is calculated. Taking into account a site change process of Cu^{2+}- and Fe^{3+}-ions forming $[Cu^{1+}_{0.06}Fe^{3+}_{0.94}][Cu^{2+}_{0.84}Fe^{3+}_{1.16}]O_{4.02}$, $n_B = 1.94$ results. The experimental value $n_B = 2.1$ determined at 5 K correlates with a composition $[Cu^{1+}_{0.06}Cu^{2+}_{0.02}Fe^{3+}_{0.92}][Cu^{2+}_{0.82}Fe^{3+}_{1.18}]O_{4.02}$. Like this, we can also induce significant changes in σ_S and n_B for the other compositions by small changes in the oxidation state of copper within the phase width of the spinel.

3.3.2. *Nickel containing copper ferrites "$Cu_xNi_{1-x}Fe_2O_4$; $x = 0.3$, 0.5, 0.6, 0.7, 0.9"*

First of all, spinel phases obtained from the decomposition of the freeze dried Ni(II)–Fe(III) formate with Ni:Fe = 1:2 were characterized. The saturation magnetization (σ_S) value of ~5.45 emu/g obtained for a single phase

TABLE II Magnetic properties and lattice parameters of copper ferrite samples

Composition	Synthesis conditions	Magnetization at 5 K σ_S (emu/g)	n_B (μ_B)	Lattice parameter "a" (pm)
$Cu_{0.9}Fe_{2.1}O_4$	1000°C, air	49.8	2.1	584.7 (c = 858.9)
$Cu_{0.8}Fe_{2.2}O_4$	1000°C, air	70.9	3.0	839.5
$Cu_{0.67}Fe_{2.33}O_4$	1100°C, argon 4.6 + 1% O_2	125.4	5.3	840.2
$Cu_{0.6}Fe_{2.4}O_4$	1100°C, argon 4.6 + 1% O_2	126.6	5.4	840.9
$Cu_{0.5}Fe_{2.5}O_4$	1110°C, argon 4.6	153.3	6.5	841.1

TABLE III Magnetic properties of quenched $Cu_xNi_{1-x}Fe_2O_4$ ferrite samples

	Magnetization at 5 K		Magnetization at 300 K	From [4]	
Composition	σ_S (emu/g)	$n_B(\mu_B)$	σ_S (emu/g)	$n_{(B)}$ ($\mu_{(B)}$), extrapol.to 0 K	σ_S (emu/g) at 300 K
$NiFe_2O_4$			46.9	2.182	47.15
$Cu_{0.3}Ni_{0.7}Fe_2O_4$	62.4	2.6	44.0	2.112	44.79
$Cu_{0.5}Ni_{0.5}Fe_2O_4$	60.9	2.6	43.5	2.216	44.99
$Cu_{0.6}Ni_{0.4}Fe_2O_4$	–	–	42.8	2.263	47.30
$Cu_{0.7}Ni_{0.3}Fe_2O_4$	58.1	2.5	46.5	2.279	45.50
$Cu_{0.9}Ni_{0.1}Fe_2O_4$	–	–	47.2	2.246	44.03

$NiFe_2O_4$, prepared at 400°C, increases up to 43.6 emu/g while nickel ferrite is prepared at 1000°C (3 h). Moreover, the increase of σ_S is noticeable when the annealing time used at 1000°C increases. The saturation magnetization value of 46.9 emu/g at room temperature obtained for a sample which is prepared at 1000°C during 24 h is close to values between 47 and 56 emu/g, obtained using the ceramic method [4, 20]. That means, the preparation of a single phase nickel ferrite at low temperature is an advantage only in a qualified sense. The formation of nickel ferrite with optimum magnetic properties requires conditions similar to these of the solid state reaction. For the investigated copper nickel ferrites, the values of σ_S at 5 K and 300 K and the calculated magnetization numbers n_B are shown in Table III. This table includes some results of Kiran and coworkers [4]. In [4], nickel copper ferrite powders were prepared from the respective oxides. After heating at 1050°C during 24 h, the samples were also quenched to room temperature.

Contrary to the results obtained for copper ferrites (Table II), σ_S and n_B do not show a well defined dependence on the nickel concentration. A similar less significant dependence of σ_S on the composition of $Cu_xNi_{1-x}Fe_2O_4$—spinels is found by Hoque *et al.* [21]. The authors discuss a shallow maximum at $x = 0.2$ as an influence of sinterability during the synthesis at 1250°C. Both Cu^{2+} and Ni^{2+} ions prefer octahedral places. Consequently, for a solid solution row $Cu_xNi_{1-x}Fe_2O_4$ of inverse or nearly inverse spinels a continious decrease of σ_S and n_B could be expected with the increase of x. However, from the data in Table III and [21], σ_S and n_B hardly vary with the composition. The small difference observed between our data and the data of [4] and [21] may be due to the difference in the method of synthesis and to the different conditions of firing. Consequently, for the same composition, the generated cations distribution should be a little different. Nickel ions have the strongest preference for octahedral sites. The cation distribution of nickel ferrite (mother compound) obtained from the magnetization data is close to $(Fe)_A[NiFe]_BO_4$. Because of a small orbital momentum contribution the magnetic moment of Ni^{2+} in ferrimagnets is $n_B = 2.18$ [4]. To explain the magnetization data of $Cu_xNi_{1-x}Fe_2O_4$ compounds, the cations distribution "$(Cu^{2+}{}_yFe^{3+}{}_{1-y})_A[Ni^{2+}{}_{1-x}Cu^{2+}{}_{x-y}Fe^{3+}{}_{1+y}]_BO_4$" is mostly proposed. For a defined composition, the higher the value of y (amount of copper ions in the A-sites), the higher becomes the magnetization number (n_B). In fact, the presence of the Cu^{2+} ions in the A-sites displaces the same amount of Fe^{3+} ions towards the *B*-sites. This influence can compensate the decrease of the magnetization by the substitution of Ni^{2+} by Cu^{2+}. Consequently, the resultant magnetization number can remain constant.

All the n_B values given in Table III for samples with $x < 0.7$ can be calculated with an occupation factor of $y \approx 0.1$ for copper ions on A-sites. The presence of appropriate amounts of Cu^+ during the preparation at 1000°C is very likely. Cu^+ should occupy only the A-sites. Its oxidation during the cooling process should be easier than the site change process. It follows that this fact could be the main reason for the formation of copper containing spinel ferrites with different cation distribution and therefore different magnetic properties in dependence on the reaction temperature and the cooling rate. The samples $Cu_xNi_{1-x}Fe_2O_4$ with $x \geq 0.7$ contain an iron rich spinel phase and a small amount of CuO. If we assume that the spinel phase in these samples has a composition close to the section $Cu_{0.6}Ni_{0.4}Fe_2O_4$–$Cu_{0.9}Fe_{2.1}O_4$ (Fig. 5), occupation factors for copper ions on A-sites of $y \approx 0.1$ are also sufficient to explain the experimental magnetization values given in Table III. For instance, if we assume that a sample with the composition "$Cu_{0.9}Ni_{0.1}Fe_2O_4$" gives a spinel phase $Cu_{0.8}Ni_{0.1}Fe_{2.1}O_4$ at 1000°C (reaction 2) a n_B value of 2.42 can be calculated.

$$1.05Cu_{0.9}Ni_{0.1}Fe_2O_4 \rightarrow 0.15CuO + 0.025O_2$$
$$+[Cu^{1+}{}_{0.1}Fe^{3+}{}_{0.9}][Cu^{2+}{}_{0.7}Ni^{2+}{}_{0.1}Fe^{3+}{}_{1.2}]O_4$$

Probably, the results of [21] can be interpreted in a similar manner. The authors discuss single phase spinels, but the XRD pattern of the copper rich compounds also refer to the presence of some copper oxide.

4. Conclusion

The thermal decomposition of freeze dried formate precursors is a suitable method for preparing copper nickel ferrites $Cu_xNi_{1-x}Fe_2O_4$ with $0 \leq x < 0.7$. In comparison with the conventional solid state reaction, the temperature necessary for the production of single phase compounds

is much lower, but the formation of optimum magnetic properties requires conditions similar to these of the solid state reaction. Copper ferrite shows a tetragonal structure when slowly cooled from high temperature to room temperature. The replacement of Cu^{2+} with Ni^{2+} leads to the decrease of the number of the distorting Cu^{2+} on octahedral (B) sites. This reduces the tetragonal distortion of copper ferrite and brings it to a cubic structure. As previously shown elsewhere for iron rich copper ferrites [8], the synthesis of iron-rich copper nickel ferrites $Cu_{0.5+y}Ni_{0.5-y-z}Fe_{2+z}O_{4\pm}$, $0 \leq (y + z) \leq 0.5$ in the phase triangle $Cu_{0.5}Ni_{0.5}Fe_2O_4$–$CuFe_2O_4$–$Cu_{0.5}Fe_{2.5}O_4$ requires specific temperature—$p(O_2)$ conditions. The study of consequences resulting from the oxygen exchange between the ferrite powders and a reducing gaseous phase as well as the electrical properties measurements have proven that the oxygen non-stoichiometry δ and the stability of copper containing ferrites strongly depend on the temperature and on the $p(O_2)$ of the gaseous phase. For a fixed metal ion ratio, the non stoichiometry δ is only about ± 0.03. Significant changes in the oxygen content lead to the separation in different phases.

For the ferrite samples, it is well established that the temperature affects the mobility of the charge carriers but not their concentration. However in the case of copper ferrite samples, one notes that a great number of processes occurring with the variation in the temperature can affect the number of charge carriers. The most common processes are the change of the composition of copper ferrite as function of the temperature and the change of the distribution of cation according to the cooling and heating rates.

Acknowledgments

The authors would like to thank Prof. Dr. H. Ullmann for helpful discussions and for giving the opportunity to use the OXYLYT-Solid Electrolyte apparatus. Dr. M. Al Daroukh is acknowledged for the measurement of the thermodynamic stability and the electrical conductivity. Thanks are also given to Dr. Mathias Doerr for magnetic measurements.

References

1. I. G. VAN UITERT, *J. Appl. Phys.* **27** (1956) 723.
2. P. MUTHUKUMARASAMY, T. NAGARAJAN and A. NARAYANASAMY, *J. Phys. C: Sol. Stat. Phys.* **15** (1982) 2519.
3. W. C. KIM and S. J. K. KIM and C. S. KIM, *J. Magn. Magn. Mater.* **239** (2002) 82.
4. H. V. KIRAN, A. L. SHASHIMOHAN, D. K. CHAKRABARTY and A. B. BISWAS, *Phys. Status Solidi A* **66** (1981) 743.
5. A. M. SANKPAL, A. R. SAWANT and A. S. VAINGANKAR, *Indian J. Pure & Appl. Phys.* **26** (1988) 459.
6. H. LANGBEIN and S. CHRISTEN, G. BONSDORF, *Thermochim. Acta* **327** (1999) 173.
7. F. KENFACK and H. LANGBEIN, *ibid.* **426** (2005) 61.
8. *ibid. Cryst. Res. Technol.* **39** (2004) 1070.
9. *ibid. Cryst. Res. Technol.* (submitted).
10. G. BONSDORF, M. A. DENECKE and K. SCHÄFER, S. CHRISTEN, A. LANGBEIN and W. GUNßER, *Solid State Ionics* **101–103** (1997) 351.
11. *Powder Diffraction Software for Data collection and Data Evaluation* (Stoe & Cie GmbH, Darmstadt, 1999).
12. M. BODE, K. TESKE and H. ULLMANN, *G.I.T. Fachzeitschr. Lab.* **5** (1994) 495.
13. D. RAVINDER, *Mater. Lett.* **43** (2000) 129.
14. V. V. PARFENOV and R. A. NAZIPOV *Neorg. Mat. (Russ.)* **38** (2002) 90.
15. D. RAVINDER, G. R. KUMAR and Y. C. VENUDHAR, *J. Alloys Compds.* **363** (*2004*) *6*.
16. D. RAVINDER, *ibid.* **291** (1999) 208.
17. R. G. KULKARNI, B. S. TRIVEDI, H. H. JOSHI and G. J. BALDA, *J. Magn. Magn. Mater.* **159** (1996) 375.
18. K. TESKE, M. AL DAROUKH, H. LANGBEIN and H. ULLMANN, *Solid State Ionics* **133** (2000) 121.
19. J. SMITH and J. WIJN, in " Ferrites" (N. V. Philips Gloeilampenfabriken, 1962).
20. B. VISWANATHAN and V. R. K. MURTHY, in "Ferrite Materials Science and Technology" (Narosa Publishing House, 1990).
21. S. M. HOQUE, M. A. CHOUDHURY and M. F. ISLAM, *J. Magn. Magn. Mater.* **251** (2002) 292.

Received 18 August
and accepted 18 August 2005